iScience

Article

Rapid identification of key antibiotic resistance genes in *E. coli* using high-resolution genome-scale CRISPRi screening

Graphical abstract

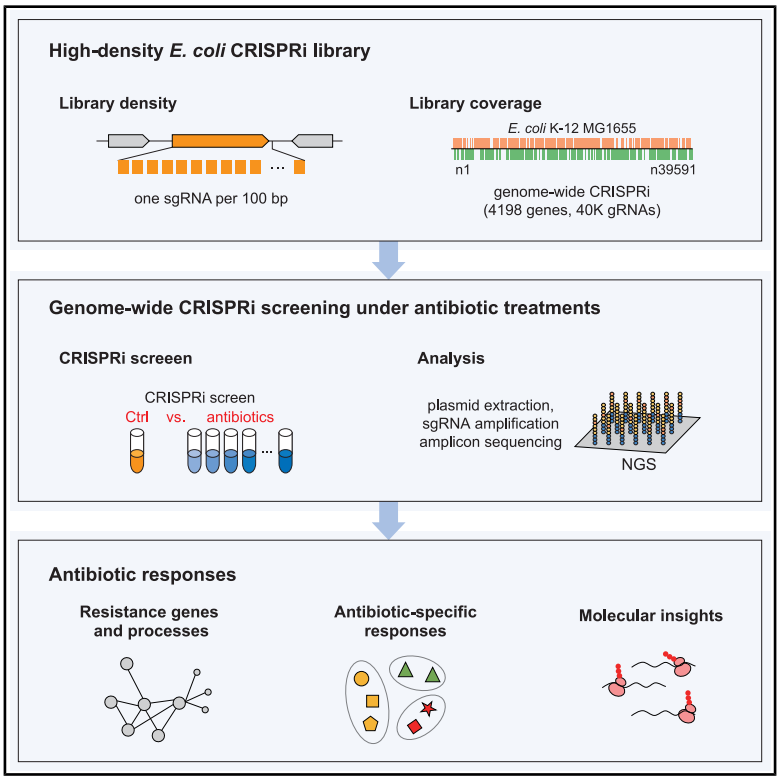

Highlights

- A high-density gRNA library was generated to target every 100 bp of the *E. coli* CDS
- Genome-wide CRISPRi reveals essential genes for antibiotic resistance and survival
- CRISPRi screening uncovers mechanisms of antibiotic resistance and susceptibility

Authors

Donghui Choe, Eunju Lee, Kangsan Kim, ..., Bernhard O. Palsson, Byung-Kwan Cho, Suhyung Cho

Correspondence

bpalsson@ucsd.edu (B.O.P.), bcho@kaist.ac.kr (B.-K.C.), shcho95@kaist.ac.kr (S.C.)

In brief

Genetics; Molecular biology; Microbiology

Choe et al., 2025, iScience *28*, 112435
May 16, 2025
https://doi.org/10.1016/j.isci.2025.112435

CellPress

iScience

CellPress
OPEN ACCESS

Article

Rapid identification of key antibiotic resistance genes in *E. coli* using high-resolution genome-scale CRISPRi screening

Donghui Choe,[1] Eunju Lee,[2,3] Kangsan Kim,[2,3] Soonkyu Hwang,[2,3] Ki Jun Jeong,[3,4,5] Bernhard O. Palsson,[1,6,*] Byung-Kwan Cho,[2,3,5,*] and Suhyung Cho[3,7,*]

[1]Department of Bioengineering, University of California, San Diego, La Jolla, CA 92093, USA
[2]Department of Biological Sciences, Korea Advanced Institute of Science and Technology, Daejeon 34141, Republic of Korea
[3]KI for the BioCentury, Korea Advanced Institute of Science and Technology, Daejeon 34141, Republic of Korea
[4]Department of Chemical and Biomolecular Engineering, Korea Advanced Institute of Science and Technology, Daejeon 34141, Republic of Korea
[5]Graduate School of Engineering Biology, Korea Advanced Institute of Science and Technology, Daejeon 34141, Republic of Korea
[6]Department of Pediatrics, University of California, San Diego, La Jolla, CA 92093, USA
[7]Lead contact
*Correspondence: bpalsson@ucsd.edu (B.O.P.), bcho@kaist.ac.kr (B.-K.C.), shcho95@kaist.ac.kr (S.C.)
https://doi.org/10.1016/j.isci.2025.112435

SUMMARY

Bacteria possess a vast repertoire of genes to adapt to environmental challenges. Understanding the gene fitness landscape under antibiotic stress is crucial for elucidating bacterial resistance mechanisms and antibiotic action. To explore this, we conducted a genome-scale CRISPRi screen using a high-density sgRNA library in *Escherichia coli* exposed to various antibiotics. This screen identified essential genes under antibiotic-induced stress and offered insights into the molecular mechanisms underlying bacterial responses. We uncovered previously unrecognized genes involved in antibiotic resistance, including essential membrane proteins. The screen also underscored the importance of transcriptional modulation of essential genes in antibiotic tolerance. Our findings emphasize the utility of genome-wide CRISPRi screening in mapping the genetic landscape of antibiotic resistance. This study provides a valuable resource for identifying potential targets for antibiotics or antimicrobial strategies. Moreover, it offers a framework for exploring transcriptional regulatory networks and resistance mechanisms in *E. coli* and other bacterial pathogens.

INTRODUCTION

Bacteria exhibit remarkable adaptability to diverse environments, primarily due to their acquisition and optimization of various gene sets throughout evolution. However, our incomplete understanding of gene functions hinders the precise identification of genes responsible for specific adaptive responses. By assessing gene essentiality under various conditions, we can identify genes and cellular processes that help bacteria withstand particular stresses. This knowledge is crucial for understanding key genetic functions at a molecular level, enabling biotechnological applications, and combating drug-resistant pathogens.

Traditionally, gene essentiality has been studied using methods such as gene knockouts[1] and transposon-mediated gene inactivation.[2] While effective for identifying genes whose disruption is lethal, these techniques struggle to detect genes that are important but not critical for survival. Recently, clustered regularly interspaced short palindromic repeat interference (CRISPRi) has emerged as a powerful tool for investigating gene essentiality through transcriptional inhibition without gene disruption.[3,4] When combined with high-throughput sequencing and a pooled library of single guide RNAs (sgRNAs), CRISPRi enables genome-wide identification of essential genes with high sensitivity and minimal background noise.[5,6] The use of a pooled library of sgRNAs, each targeting different regions of multiple genes, further enhances the effectiveness of this approach for a broad range of applications.[7,8]

Transcriptome profiling is another method used to study bacterial responses to antibiotics by examining gene expression levels under stress.[9] However, this approach is limited to identifying genes already programmed to respond to antibiotic stress in the specific bacteria of interest and is typically used to explore resistance mechanisms in known antibiotic-resistant strains. In contrast, CRISPRi not only identifies genes directly involved in resistance mechanisms but also uncovers genes that might influence antibiotic tolerance and potentially evolve into resistance mechanisms, providing a broader perspective on bacterial adaptation.

In this study, we designed a high-density sgRNA library targeting the entire coding sequence (CDS) of *Escherichia coli* K-12 MG1655. By monitoring changes in sgRNA populations within

bacterial cultures exposed to various antibiotics, we rapidly identified genes involved in antibiotic responses. Our CRISPRi screen demonstrated advantages over conventional methods, particularly in its ability to identify essential genes without completely disrupting their function. This approach provided insights into cellular targets of antibiotics, including those with poorly understood molecular mechanisms.

RESULTS

Genome-wide fitness effect of a gene knockdown using high-resolution CRISPRi screening

We adopted the CRISPRi system to probe the fitness effect of gene knockdown in *E coli* K-12 MG1655.[4,10] The system, comprising two plasmids expressing dCas9 and sgRNA, efficiently inhibited the expression of monomeric red fluorescent protein (*mrfp*) encoded in the *E. coli* genome (Figures S1A and S1B). CRISPRi-mediated inhibition of essential genes (*groS* and *rpoD*) decreased growth rates and extended lag phases (Figure S1C), while knockdown of non-essential genes (*pfkB* and *rpoS*) produced no significant changes. The varying levels of growth retardation induced by *groS* and *rpoD* knockdown indicated different fitness effects, a nuance not observable in gene knockout studies.

To investigate the fitness effects of all *E. coli* genes, we designed and synthesized a library of evenly spaced sgRNAs targeting every 100 bp of the 4,198 coding sequences (CDSs) in *E. coli* (targeting 39,591 positions, Figure 1A) (see STAR Methods). Of the sgRNAs, 39,574 sgRNA sequences were present in the initial library (lib), representing 99.96% coverage (Table S1). More importantly, the sgRNAs were uniformly represented in the library, as 99% of sgRNAs were observed less than 3.6 times when 39,591 reads were observed (median of 0.7 times per 39,591 reads) (Figure S2A). We then transformed this library into *E. coli* expressing dCas9 and cultured the cells under various antibiotic conditions. Under these conditions, cells with deleterious knockdowns exhibited reduced fitness, leading to decreased abundance. To quantify these fitness effects, we measured sgRNA abundance in the culture using next-generation sequencing and compared it to the lib. Fitness effects were quantified using the enrichment ratio (ER), a metric defined as the median ratio of all sgRNAs targeting a gene, comparing their abundance in the knockdown condition (with dCas9) to their abundance in the lib (STAR Methods, Figure 1B; Table S2).

We first analyzed sgRNA abundance in cells cultured in LB media for known essential and non-essential genes, as determined by a previous single-gene knockout study (Figure 1C).[1] Non-essential genes showed much higher ERs (median 0.989) than essential genes (median 0.346), confirming that ER accurately reflects gene knockdown fitness effects. This high-density CRISPRi approach, combined with the ER metric—which represents the median changes of multiple sgRNA targeting a single gene—offers the advantage of being robust against outliers, such as sgRNAs with low inhibitory efficiency or off-target bindings. For instance, ERs for the RNA polymerase beta and beta′ subunits, encoded by *rpoB* and *rpoC*, respectively, consistent with their critical roles in cell survival, despite the presence of sgRNAs whose abundance changes deviated from the majority targeting the same gene (Figure S2B).

To evaluate the influence of sgRNA position on inhibitory effects, we analyzed positional abundance changes of sgRNAs based on their relative positions within genes. No differences were observed when comparing sgRNA abundances in LB vs. the initial library (Figure S2C), suggesting that CRISPRi inhibitory activity remained consistent regardless of the sgRNA binding position. Additionally, we examined sgRNAs targeting 252 essential CDSs (>400 bp) to further assess positional effects. If such effects were significant, sgRNAs targeting the 5′-portion of these essential genes would show greater depletion compared to those targeting the 3′-portion. However, our analysis revealed no statistical differences in the abundance change distribution among these sgRNAs (Figure S2D), indicating consistent activity across the gene body, which align with previous findings.[6,11]

Next, we exposed the culture to sub-inhibitory concentrations of 12 different antibiotics to identify genes affecting cellular responses to antibiotics (Figure S3; Table S3): (1) oxidative phosphorylation inhibitor carbonyl cyanide 3-chlorophenylhydrazone (CCCP), (2) polymyxin B outer membrane destabilizer, (3) pyocyanin redox stress inducer, (4) transcription inhibitor rifampicin, (5) folate biosynthesis inhibitor sulfamethizole, (6) calcium channel blocker verapamil, two translational inhibitors, erythromycin and puromycin, and (7) four DNA damage inducers—phleomycin, mitomycin C, methyl methanesulfonate (MMS), and novobiocin.

Universal responses of *E. coli* against various antibiotic treatments

Principal component analysis (PCA) of the ER data revealed diverse responses of *E. coli* to antibiotics with different modes of action (Figure 2A). The analysis showed a diverse distribution of conditions, indicating that the enrichment of knockdown strains in the culture population varied depending on the antibiotics used. Although the *E. coli* strain was sensitive to all antibiotics tested, changes in sgRNA abundance following antibiotic exposure showed that certain gene knockdowns were either advantageous or detrimental to cell survival at sub-lethal antibiotic concentrations.

To identify significant gene knockdowns, we compared the ERs of individual genes and their fold changes between treated and untreated controls. Genes with an ER that changed by more than 1.5-fold compared to the untreated control and with an average ER above 0.25 were considered to significantly affect fitness under a given antibiotic treatment. As a result, 1,085 gene knockdowns were found to induce significant fitness differences in response to antibiotics (Table S4). The majority of these knockdowns (72.9%) were specific to only one or two antibiotics, while a small subset of genes had pleiotropic effects across multiple antibiotics (Figure S4).

Before investigating individual genes responding to each antibiotic, we aimed to determine whether there was a universal set of genes in *E. coli* that respond to various antibiotics. Interestingly, seven genes exhibited consistent changes in their ERs across 10 or more antibiotics (Figure 2B). The stress response sigma factor RpoS, known for its involvement in various antibiotic responses, did not meet this criterion, as it showed

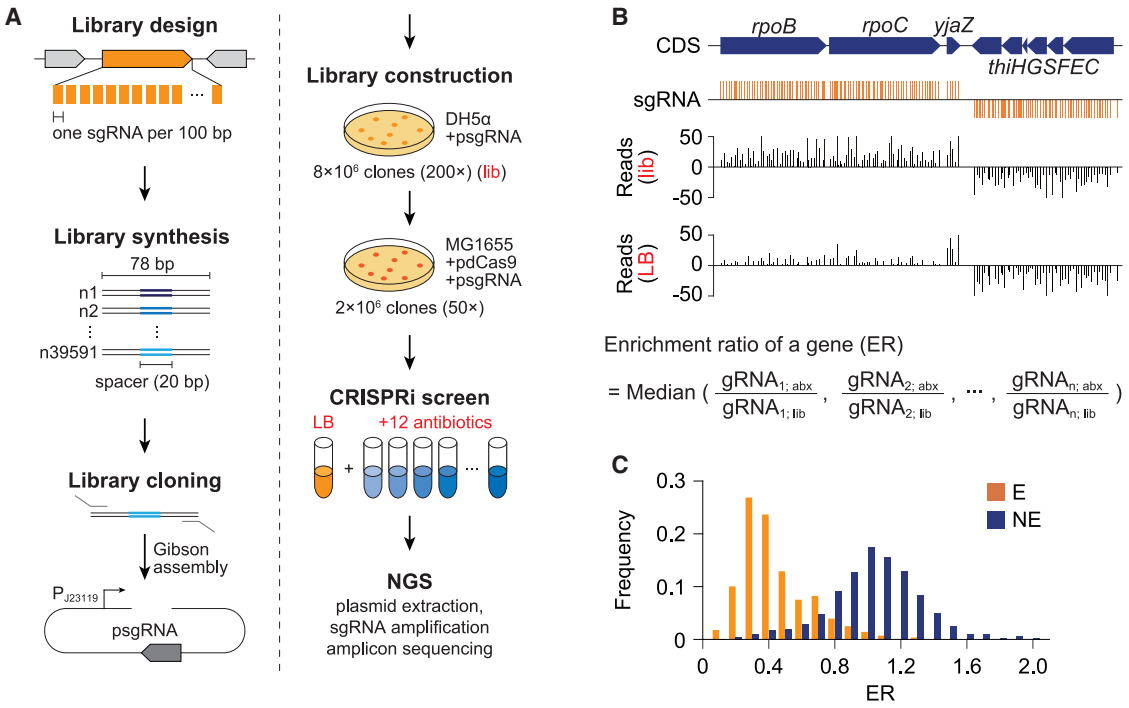

Figure 1. Genome-scale CRISPRi screen

(A) Schematic of library design and construction for genome-scale CRISPRi screening following various antibiotic treatments using a sgRNA library (lib) (n = 39,591) that targeted every 100 bp of coding sequences in *E. coli*.

(B) Profiles of sgRNA abundance in a synthetic library (lib) and genome-scale CRISPRi screening. The number of each sgRNA was normalized by the number of million mapped reads. The enrichment ratio (ER) of a gene was defined as the median abundance change of individual sgRNAs in a gene.

(C) ER distribution of known essential (E) and non-essential (NE) genes based on single gene knockout study.[1] See also Figures S1–S3, Tables S1, S2, and S3.

significant ER changes in response to eight antibiotics (Figure 2B). Compared to RpoS, the broad-spectrum fitness effects of these seven genes were unexpected.

Knockdowns of three of these universally responding genes—*degP*, *yacG*, and *ybbC*—resulted in deleterious fitness effects under antibiotic treatments, suggesting their protective roles against antibiotics. *degP* encodes the protease Do, which degrades abnormal, damaged, and aggregated proteins in the periplasm.[12–14] Growth profiling of a *degP* null mutant revealed weaker growth compared to the wild-type strain when exposed to multiple antibiotics (Figures 2C and S5). Although the growth defect was not highly significant, the *degP* mutant showed a minor competitive disadvantage in the population. Given the protective effect of *degP* against antibiotic stress, its beneficial role against two translational inhibitors erythromycin and puromycin was expected. However, its prominent role against many other antibiotics was surprising. It is possible that a slower division rate requires elevated protein quality control activity or that *degP* plays a crucial role in maintaining the integrity of the membranous and periplasmic barriers, which are important for excluding or preventing the entry of toxic compounds. *E. coli* has two additional serine proteases, DegQ and DegS, which are homologous to DegP.[15] However, the ERs of these proteases did not change significantly (Table S2). DegP, DegQ, and DegS belong to the HtrA family of proteases, which are implicated in protein quality control and chaperone activity. The functional differences between these HtrA family proteases are not well understood, but there is evidence that they may have non-overlapping functions, as suggested by the inability of DegS or the partial ability of DegQ to complement the loss of DegP.[15] Differences in localization, regulatory roles, and potential substrate specificity and processivity could explain why DegP alone is responsible for the antibiotic stress response.[16]

Additionally, the population of sgRNAs targeting the endogenous gyrase inhibitor YacG[17] was depleted upon antibiotic exposure (Figure 2B). While the impact of YacG perturbation on DNA-damaging agents is understandable, its effect on antibiotics seemingly unrelated to DNA was unexpected. This may be due to reduced levels of energetically costly DNA replication and transcription, mediated by the gyrase inhibitor YacG, in non-dividing cells, resulting in a more stress-tolerant state. However, detailed molecular links between YacG and various antibiotics require further investigation. The last gene, *ybbC*, showed a drastic decrease in gRNA abundance, indicating a potential protective role in the antibiotic stress response.

On the other hand, knockdowns of the remaining four genes—*yjiG*, *rmlE*, *yebO*, and *yoaC*—had beneficial effects (Figure 2B), suggesting that their functions are detrimental for survival under antibiotic exposure. Although YebO is predicted to be located on the inner membrane, the molecular roles of YoaC and YebO in the antibiotic response remain unclear, as the functions of these proteins have not yet been characterized. However, there are

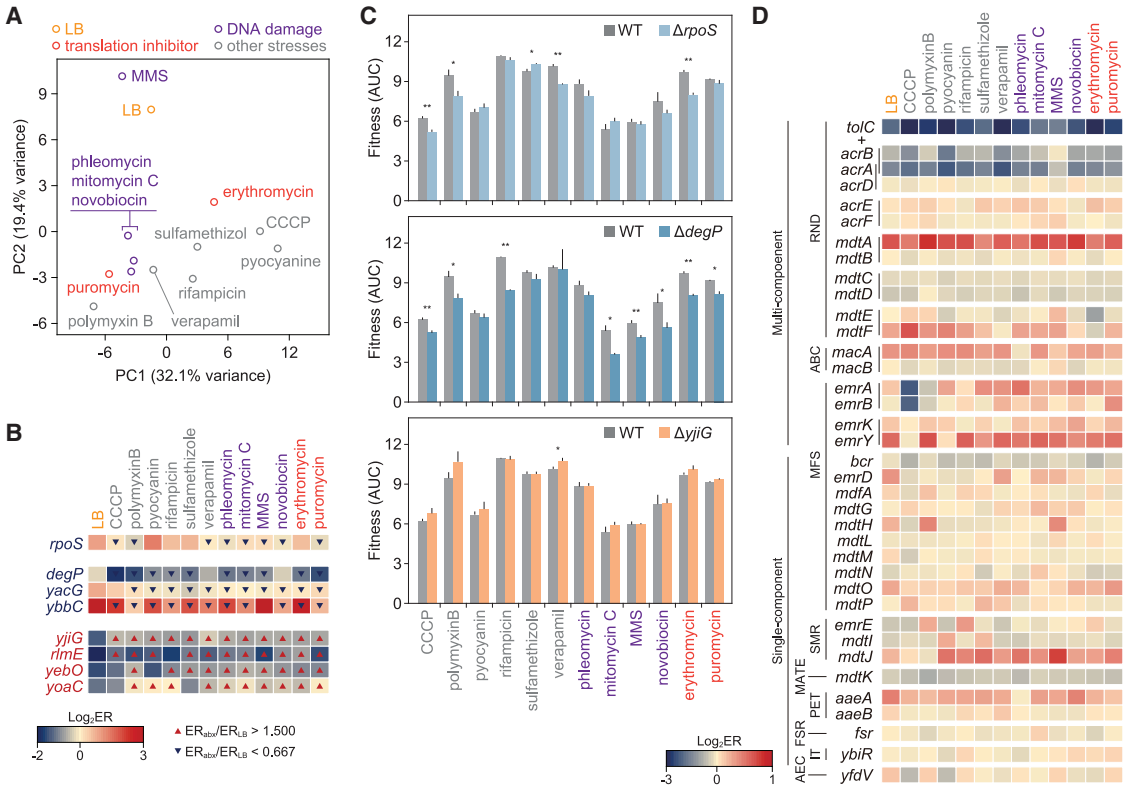

Figure 2. Changes in gene essentiality under various antibiotics treatments

(A) Principal component analysis of the various stresses was performed based on ER.

(B) Genes whose ERs changed significantly against 10 or more antibiotics. Blue and red triangles indicate ERs increased and decreased 1.5-fold, respectively, with mean ER (treatment and untreated LB control) larger than 0.25.

(C) Fitness of *rpoS*, *degP*, and *yjiG* knockout strains under antibiotics treatment. Area under growth curve (AUC) estimates growth performance, calculated from growth curve (7 h of incubation). Bars and error bars represent mean values and SD of three replicated cultures. **p*-value < 0.05, ***p*-value < 0.01 (two-sided Welch's *t*-test).

(D) Heatmap showing the ER values of genes related to multidrug resistance and efflux systems according to the stresses. RND: resistance-nodulation-division family transporters. ABC, ATP-binding cassette transporters; MFS, major facilitator superfamily transporters; SMR, small multidrug resistance family protein; MATE, multidrug and toxic compound extrusion family transporters; PET, putative efflux transport family transporters; FSR, fosmidomycin resistance family protein; IT, ion transporter superfamily transporter; AEC, auxin efflux carrier family transporter. See also Figures S4, S5, Tables S2, and S4.

potential explanations for the deleterious effects observed in the knockdowns of *yjiG* and *rmlE*. YjiG is a Gate family protein located in the periplasm with predicted inner membrane domains.[18] The protein belongs to two protein families: the FeoB GTPase Gate (InterPro: IPR011642) and spore maturation protein B (SmpB; InterPro: IPR052549) families. The Gate domain is responsible for nucleoside specificity in human nucleoside transporter proteins,[19] while in bacteria, it functions in Fe^{2+} transport.[20] Thus, this domain may be involved in the transport of a wide range of substrates. Additionally, the SmpB family includes proteins involved in transporting various molecules in or out of spores. Based on the CRISPRi screening and the functions of the protein domains, we predict that YjiG functions as a gate, potentially serving as an entry point for antibiotics. To further investigate this hypothesis, we monitored the growth of an *yjiG* knockout strain under antibiotic treatment (Figures 2C and S5). Although the fitness increase was not highly significant, the absence of YjiG enhanced the fitness of *E. coli* against most antibiotics (Figure 2C), supporting our hypothesis.

Lastly, *rlmE* encodes a 23S rRNA 2′-*O*-ribose U2552 methyltransferase, which does not appear to be directly related to antibiotic response. However, previous studies have shown that disruption of genes involved in RNA modification can be either detrimental or beneficial,[21,22] potentially due to differential translation and codon adaptation that affect bacterial stress response. Specifically, *rlmE* disruption had beneficial effects under sub-lethal levels of tobramycin and ciprofloxacin in *Vibrio cholerae*.[23] The molecular connections between antibiotics and translational adaptations through RNA modification are intriguing and warrant further in-depth investigation.

Additionally, several mechanisms, including efflux pumps, have been reported in *E. coli* that confer protection against a wide range of stresses and chemicals.[24,25] We found that the outer membrane channel TolC exhibited a lower ER when treated with most antibiotics compared to the LB control, indicating its versatile role in cellular defense (Figure 2D). Notably, the ER of *tolC* (0.245) in the LB control was below the median ER of essential genes (0.346), consistent with the previously

Table 1. Summary of genes exhibited significant ER changes upon antibiotic treatments

Antibiotics	Gene	Description	ER change
Pyocyanin	*soxRS*	DNA-binding transcriptional dual regulators SoxR	Decreased
	ubiC	chorismate lyase	Decreased
	ubiD	3-octaprenyl-4-hydroxybenzoate decarboxylase	Decreased
	ubiF	3-demethoxyubiquinol 3-hydroxylase	Decreased
	ubiH	2-octaprenyl-6-methoxyphenol 4-hydroxylase	Decreased
	ubiI	2-octaprenylphenol 6-hydroxylase	Decreased
	ubiX	flavin prenyltransferase	Decreased
	yqiC	ubiquinone biosynthesis accessory factor UbiK	Decreased
	sufA	iron-sulfur cluster insertion protein SufA	Decreased
	sufBCD	Fe-S cluster scaffold complex	Decreased
	sufE	sulfur carrier protein SufE	Decreased
	sufS	L-cysteine desulfurase	Decreased
	arcA	DNA-binding transcriptional dual regulator ArcA	Decreased
	iscS	cysteine desulfurase	Decreased
	gshA	glutamate—cysteine ligase	Increased
	gshB	glutathione synthetase	Increased
	gss	fused glutathionylspermidine amidase/glutathionylspermidine synthetase	Increased
	sapA	putative periplasmic binding protein SapA	Increased
	sapBC	putrescine ABC exporter membrane subunits	Increased
	sapDF	putrescine ABC exporter ATP binding proteins	Increased
CCCP	*yoaI*	predicted small protein YoaI	Decreased
	ybhF	ABC exporter ATP binding subunit YbhF	Decreased
	ybhG	HlyD_D23 family protein YbhG	Decreased
	ybhSR	putative ABC exporter membrane subunits	Decreased
	ybiH	DNA-binding transcriptional dual regulator CecR	Decreased
	atpB	ATP synthase Fo complex subunit a	Decreased
	nuoBEGHJKLM	NADH:quinone oxidoreductase	Decreased
	cyoA	cytochrome bo_3 subunit 2	Decreased
	cydAB	cytochrome bd-I subunits	Decreased
	sdhACE	succinate:quinone oxidoreductase	Decreased
	hpf	ribosome hibernation-promoting factor	Increased
	sapA	putative periplasmic binding protein SapA	Increased
	sapBC	putrescine ABC exporter membrane subunits	Increased
	sapF	putrescine ABC exporter ATP binding proteins	Increased
Polymyxin B	*waaB*	UDP-D-galactose:(glucosyl)lipopolysaccharide-1,6-D-galactosyltransferase	Decreased
	waaC	ADP-heptose:LPS heptosyltransferase 1	Decreased
	waaO	UDP-D-glucose:(glucosyl)LPS α-1,3-glucosyltransferase	Decreased
	waaP	lipopolysaccharide core heptose (I) kinase	Decreased
	waaQ	lipopolysaccharide core heptosyltransferase 3	Decreased
	waaR	UDP-glucose:(glucosyl)LPS α-1,2-glucosyltransferase	Decreased
	waaZ	lipopolysaccharide core biosynthesis protein	Decreased
	bamACE	outer membrane protein assembly factors	Decreased
	pldA	outer membrane phospholipase A	Decreased
	opgGH	osmoregulated periplasmic glucans biosynthesis proteins	Decreased
	tolR, pal	Tol-Pal system proteins	Decreased

(*Continued on next page*)

Table 1. *Continued*

Antibiotics	Gene	Description	ER change
Rifampicin	*rpoD*	RNA polymerase sigma factor	Decreased
	rraA	ribonuclease E inhibitor protein A	Decreased
	sapA	putative periplasmic binding protein SapA	Increased
	sapBC	putrescine ABC exporter membrane subunits	Increased
	sapDF	putrescine ABC exporter ATP binding proteins	Increased
Sulfamethizole	*folB*	dihydroneopterin aldolase	Decreased
	folK	2-amino-4-hydroxy-6-hydroxymethyldihydropteridine diphosphokinase	Decreased
	nudB	dihydroneopterin triphosphate diphosphatase	Decreased
	folD	bifunctional methylenetetrahydrofolate dehydrogenase/ methenyltetrahydrofolate cyclohydrolase	Increased
	sapA	putative periplasmic binding protein SapA	Increased
	sapBC	putrescine ABC exporter membrane subunits	Increased
	sapF	putrescine ABC exporter ATP binding proteins	Increased
Verapamil	*secF, yajC*	Sec translocon accessory complex subunit	Decreased
	tolAQR, pal	Tol-Pal system proteins	Decreased
	mlaCDE	intermembrane phospholipid transport system proteins	Decreased
	tatAC	twin arginine protein translocation system proteins	Decreased

See also, Table S4.

observed growth defect of the *tolC* mutant, underscoring its physiological importance.[26,27] TolC forms a tripartite efflux pump with resistance-nodulation-division (RND) partners, consisting of a membrane fusion protein (MFP) and a permease, such as AcrAB and MdtEF.[28] In response to erythromycin, the mean ER of *mdtE*, *mdtF*, and *tolC* decreased to 53.8% of that in LB (ER_{LB}) (Figure 2D). MdtEF has been reported as an efflux pump for erythromycin,[29] thus validating the CRISPRi-based identification of genes involved in the antibiotic stress response. Interestingly, the ER of the MFP component MdtE decreased by 1.33-fold with pyocyanin treatment compared to ER_{LB}, whereas its known permease partner, MdtF, was resistant to CRISPRi knockdown. In fact, MFP-permease complexes can form chimeric structures with different partners,[30,31] resulting in different substrate specificities. Similarly, MdtE may interact with an orthologous permease to exclude pyocyanin.

In addition to MdtEF, the *E. coli* AcrA mutant has also been shown to be susceptible to mitomycin C, erythromycin, and novobiocin[32]; however, the ERs for the three drug treatments were marginal in the CRISPRi screen (90.0, 91.2, and 100.1% of ER_{LB}, respectively). This may indicate the presence of redundant efflux pumps that mitigate the knockdown effect of AcrA. Furthermore, pyocyanin treatment resulted in 1.9- and 1.2-fold lower ERs for *acrAB* and the RND proton antiporter *ermKY*, respectively, compared to ER_{LB}. These results suggest a possible role for AcrAB-TolC and ErmKY-TolC in pyocyanin efflux in *E. coli*. Interestingly, the ER of *tolC* decreased by 1.3- and 1.5-fold when treated with phleomycin and puromycin, respectively. However, none of the known RND partners exhibited an ER lower than that of LB, implying the existence of unknown RND systems responsible for exporting phleomycin and puromycin. This discovery could provide insights into the diverse specificity of TolC when paired with different RND partners, potentially revealing a broader range of interactions than previously understood.

The CRISPRi screen identified genes involved in antibiotic responses that had not been previously recognized. Moreover, this approach may more accurately reflect population dynamics, closely mimicking physiological scenarios compared to single-gene disruption studies.

CRISPRi screen reveals specific cellular targets of antibiotic action

Responses to reactive oxygen species generating antibiotics: Pyocyanin

Next, we investigated how individual genes in *E. coli* change their fitness in response to various antibiotics (Table 1). First, pyocyanin, a redox-active compound, exerts its antibiotic effect by generating reactive oxygen species (ROS).[33] While its targets and mechanisms are well-established in human cells,[34,35] its molecular action in bacterial cells remains less understood. Contrary to earlier findings that pyocyanin generates ROS, the ERs of superoxide dismutase and catalase did not show significant changes, likely due to their redundant roles in ROS management.[36] Instead, the ERs of the redox-responsive two-component systems SoxRS and ArcAB decreased by 6.0- and 1.6-fold, respectively (Figure 3A). These systems are crucial for managing ROS stress by activating genes involved in ROS mitigation.[37,38] When *soxR* and *soxS* knockout mutants were tested, they exhibited significantly higher sensitivity to pyocyanin, compared to the wild-type control (Figures S6A and S6B), supporting the observed decrease in ER for the SoxRS system under pyocyanin stress.

The CRISPRi screening also revealed effects on other cellular processes. Specifically, genes involved in both iron-sulfur systems, Isc and Suf, showed decreased ERs, indicating damage

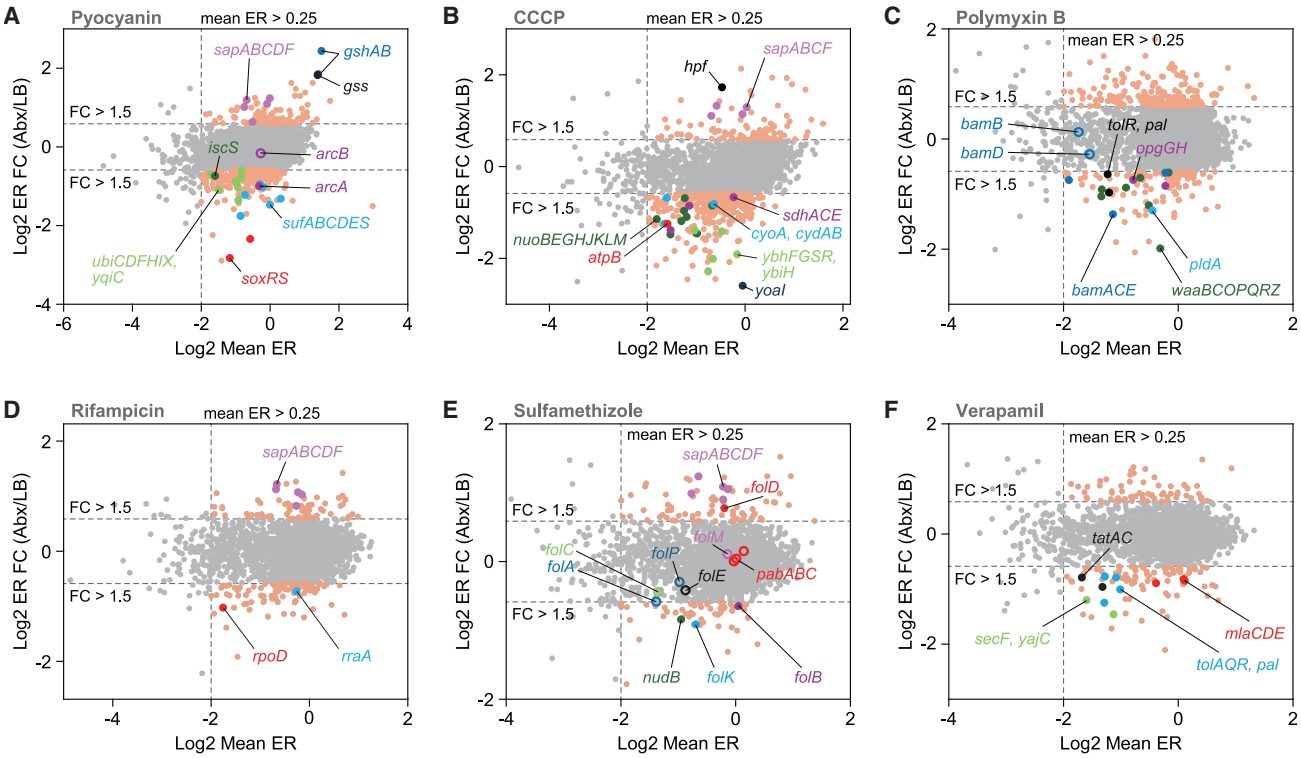

Figure 3. MA-plot (log ratio and log mean) showing genes with significant fitness effect under various antibiotics treatments

(A–F) Genes whose ERs enriched or extinct more than 1.5-fold than untreated control (horizontal dashed lines) and average ER more than 0.25 (vertical dashed lines) were chosen as significantly affecting fitness in (A) pyocyanin, (B) CCCP, (C) polymyxin B, (D) rifampicin, (E) sulfamethizole, and (F) verapamil treatments. See also Figure S6, Tables S2, and S4.

to iron-sulfur clusters. The entire Suf system (*sufABCDES*) exhibited an average ER decrease of 2.5-fold, while only *iscS* in the Isc system showed a significant 1.7-fold decrease. Among the two redundant iron-sulfur assembly systems, only the Suf system is induced by oxidative stress, and *iscS* is critical for repairing damaged iron-sulfur clusters.[39,40] These results underscore the damage caused by pyocyanin and the importance of the Suf system and IscS in responding to this damage.

Additionally, CRISPRi indicated perturbations in ubiquinol metabolism, evidenced by reduced fitness in knockdowns of ubiquinol-8 biosynthetic genes (*ubiIHFXCD* and *yqiC*, also known as *ubiK*) (Figure 3A). Ubiquinol-8 is essential for various redox-related processes, including respiration, and serves as an antioxidant against oxidative stress.[41] This finding further supports the notion that pyocyanin induces oxidative stress.

Interestingly, strains with reduced expression of genes responsible for glutathione and glutathionylspermidine biosynthesis (*gshAB* and *gss*) were enriched 4.2-fold upon pyocyanin treatment (Figure 3A). Pyocyanin can directly oxidize glutathione, leading to the formation of pyocyanin radicals and superoxide.[42] Thus, CRISPRi screening provides insights into the molecular mechanisms by which pyocyanin acts as an antibiotic by targeting the source of ROS.

Overall, this investigation demonstrates how CRISPRi reveals the mechanisms of antibiotic action and identifies key molecular players involved in antibiotic responses on a genome-wide scale.

Responses to oxidative phosphorylation inhibiting antibiotics: CCCP

CCCP, an inhibitor of oxidative phosphorylation, had the most pronounced effect on genes involved in the electron transport chain. This included NADH dehydrogenase I (*nuoBEGHJKLM*), succinate dehydrogenase (*sdhACE*), ubiquinol oxidase (both cytochrome *bo* and *bd-I*; *cyoA* and *cydAB*), and ATP synthase (*atpB*) (Figure 3B). Although not all subunits of these complexes exhibited significant changes in ER, the knockdown of most subunits was detrimental to fitness. This finding highlights the increased essentiality of genes involved in energy generation in response to CCCP.

We also identified a putative ABC exporter that may play a role in actively removing CCCP. This exporter, composed of YbhFSR, the membrane fusion protein YbhG, and their transcriptional regulator YbiH, showed a 3.58-fold decrease in gRNA abundance (Figure 3B). This exporter has been implicated in the efflux of various antibiotics, including cephalosporin, chloramphenicol, tetracycline, and cationic compounds.[43,44] Combined with the increased CCCP sensitivity observed in an *ybhG* knockout mutant (Figures S6A and S6C), these findings suggest that the YbhFGSR exporter may be involved in the export of CCCP.

Notably, the ER of a predicted small membranous protein, YoaI (34 amino acids), exhibited the most significant change, with over a 6-fold decrease compared to LB. Although the function of YoaI is not yet fully understood, it has been identified as part of the phosphate regulon in virulent *E. coli* O157:H7,[45] suggesting a potential role in phosphate and energy metabolism.

Conversely, knockdowns of *hpf* (ribosome hibernation-promoting factor), *sapA* (a periplasmic binding protein), and *sapBCF* (putrescine ABC exporter subunits) were beneficial for survival (Figure 3B). Hpf promotes persister cell formation by inactivating ribosomes and protecting them from ribonucleases under stress conditions, such as starvation.[46] Although Hpf helps in entering a persistent state and resuscitating from it by protecting ribosomes, our CRISPRi screen indicates a detrimental effect in the presence of CCCP. This suggests a dual role of bacterial persistence—beneficial under physiological stress and lethal antibiotic levels but potentially disadvantageous during competition under sub-lethal antibiotic levels.

Additionally, knockdowns of the Sap transporter (SapABCDF) were enriched. This transporter mediates putrescine export in *E. coli*.[47] However, SapA, a predicted periplasmic binding protein of the exporter, shares 90.5% and 38.1% sequence identity (BLASTP search) with homologs from *Salmonella typhimurium* and *Haemophilus influenzae*, respectively. In these organisms, the SapABCDF complex is responsible for importing small antimicrobial peptides rather than exporting putrescine.[48,49] Growth profiling of a *sapF* knockout strain revealed increased resistance not only to CCCP (Figures S6A and S6C) but also to multiple other antibiotics (Figure S6A). suggesting that the function and substrate of the Sap transport system in *E. coli* may differ from previously understood. Instead, combined with the growth profiling results, this indicates that the Sap transporter may serve as an entry point for antibiotics.

Responses to antibiotics with cationic detergent action: Polymyxin B

Polymyxin B challenge primarily depleted knockdowns of genes essential for maintaining outer membrane integrity. Specifically affected were genes involved in lipopolysaccharides (LPS) core biosynthesis (*waaBCOPQRZ*), components of the BAM complex (*bamACE*), outer membrane phospholipase A (*pldA*), components of the Tol-Pal complex (*tolR-pal*), and osmoregulated periplasmic glucans biosynthesis (*opgGH*) (Figure 3C).

Polycationic antibiotics like polymyxins initially enter bacterial cells through electrostatic interaction with negatively charged LPS, particularly via the phosphate groups of the lipid A moiety.[50] Enterobacteria typically develop resistance by attaching 4-amino-4-deoxy-L-arabinose to these phosphate groups,[51] a modification mediated by the Arn system (*arnABCDEFT*). However, the ER of the Arn system did not change significantly (Table S2), likely due to its low expression under the experimental conditions. This resistance mechanism requires activation of the latent Arn pathway by the BasSR two-component system under high iron concentration.[52,53] Instead, genes crucial for maintaining outer membrane integrity became more essential.

Knockdowns of many LPS core biosynthesis genes were detrimental during the polymyxin challenge. The LPS core oligosaccharide, attached to the lipid A moiety, is vital for membrane structure and stability.[54] Previous studies have shown that a *waaC* mutant, which lacks most of the core segment, is more sensitive to polymyxins.[55] Similarly, a *waaG* knockout mutant also showed increased sensitivity to polymyxin B (Figures S6A and S6D). Polymyxins exert their antibiotic effect by forming LPS-polymyxin crystal complexes, which physically disrupt the membrane.[55] The length of the LPS core affects the dimensions of these crystallin structures, thereby altering polymyxin sensitivity.[55] Thus, changes in the expression of LPS core biosynthetic genes were reflected in the ER changes, demonstrating their role in polymyxin response.

Other genes involved in maintaining membrane integrity, such as *pldA* (outer membrane phospholipase A), *tolR-pal* (Tol-Pal complex), and *opgGH* (osmoregulated periplasmic glucans biosynthesis), are also related to the polymyxin response. These genes are essential for the stability and function of the outer membrane.

The BAM complex, responsible for the assembly and insertion of beta-barrel proteins into the outer membrane, also showed significant ER changes. The ERs of this complex decreased by an average of 1.6-fold (Figure 3C), underscoring its critical role. Loss-of-function mutations in subunits of the BAM complex have been reported to increase outer membrane permeability, supporting this observation.[56,57] Because *bamA* is an essential gene, studying membrane biogenesis through the BAM complex typically requires specific approaches such as suppressor mutations or gene depletion.[56] In contrast, the CRISPRi screen effectively identified the complex despite its essential nature, showcasing the advantage of CRISPRi screening over conventional methods.

Responses to antibiotics with transcription inhibitor action: Rifampicin

Rifampicin treatment resulted in changes in the ERs of 160 genes. However, biological pathway and process enrichment analysis (KEGG mapping[58]) did not reveal any significant enrichment in conserved biological functions. Despite this, two notable observations were made: the housekeeping sigma factor RpoD and the ribonuclease E inhibitor RraA became more essential under rifampicin treatment (Figure 3D). Unlike *rraA*, no significant changes in the ER of RNases were observed (Table S2). Additionally, the Sap transporter, which showed beneficial effects against CCCP, also exhibited an increased ER under rifampicin treatment, and the *sapF* knockout strain displayed a slightly enhanced fitness in the presence of rifampicin (Figures S6A and S6E).

Responses to folic acid production inhibiting antibiotics: Sulfamethizole

Sulfamethizole, a sulfonamide antibiotic, inhibits dihydropteroate synthase (DHPS), an enzyme involved in folate synthesis.[59] Folates consist of three chemical moieties: *p*-aminobenzoate (pABA), a pterin ring, and poly-glutamate. pABA is synthesized from chorismate by the enzymes PabABC, while the pterin moiety is synthesized from GTP via NudB and FolBEK. DHPS, encoded by *folP*, then catalyzes the condensation of pABA with 6-hydroxymethyl-dihydropterin diphosphate, followed by addition of glutamates by FolC, producing dihydrofolate (DHF). DHF can be further reduced by FolM and FolA into tetrahydrofolate (THF), which serves as the backbone structure for various folate family coenzymes.

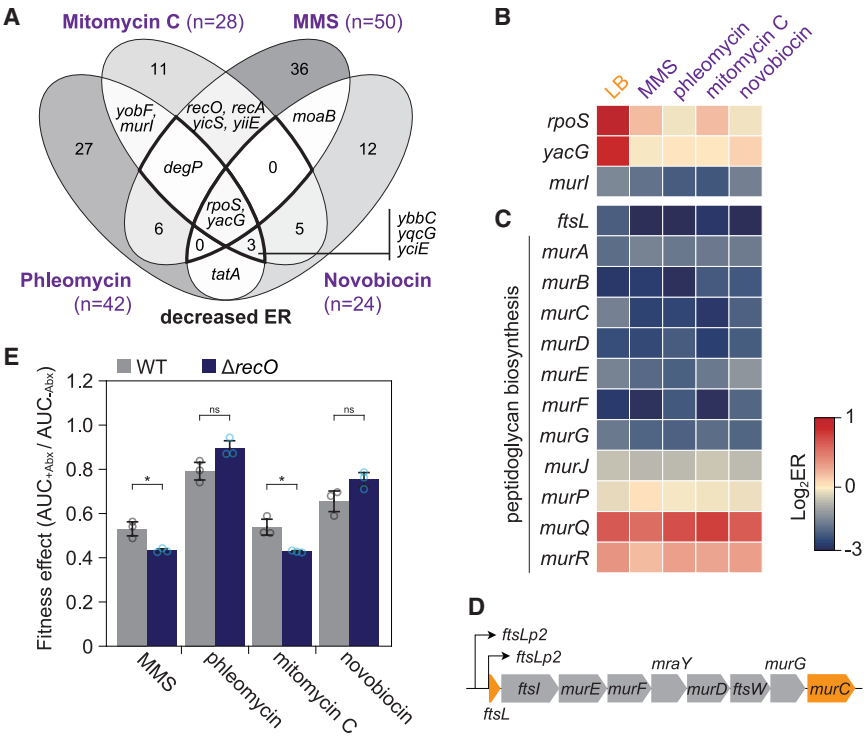

Figure 4. Genetic responses involved in DNA damage

(A) Genes with ER significantly decreased in response to DNA-damaging agents.

(B and C) Heatmaps showing the ER values of genes that are (B) essential for multiple DNA-damaging antibiotics and (C) responsible for peptidoglycan biosynthesis.

(D) Structure of the transcriptional unit containing *murC*.

(E) Fitness effects of antibiotic treatments in the wild-type or *recO* knockout strains, measured as the area under the growth curve (AUC). Fitness is defined as the ratio of AUC under antibiotic stress to AUC without antibiotics. Bars, error bars, and circles represent the mean, SD, and individual data points from three replicates, respectively. ns: no statistical difference, *p-value < 0.05 (two-sided Welch's t-test of log-transformed ratios). See also Figures S7, S8, Tables S2, and S4.

Interestingly, not all genes involved in this multi-branched folate synthesis pathway were equally affected. Genes responsible for pterin synthesis (*nudB* and *folBK*) showed a significant decrease in ER, while those involved in pABA synthesis remained unaffected (Figure 3E). The molecular target of sulfamethizole, FolP, and its downstream THF synthesis pathway (FolACM) exhibited only marginal decrease in their ERs. Additionally, FolD, which converts THF into N^{10}-formylTHF, showed a beneficial effect when knocked down in the presence of sulfamethizole (Figure 3E). The reason for the varying fitness effects among genes required for THF biosynthesis is not entirely unclear. Folates are a diverse group of compounds with varying redox states, glutamate chain lengths, and chemical modifications, serving as coenzymes in numerous cellular processes. These diverse roles may contribute to the observed differences in gene essentiality. The transformation and dynamics of folates in response to stress warrant further detailed investigation, as they may provide insights into the complex interplay between antibiotic action and cellular metabolism.

Responses to calcium-channel blockers antibiotics: Verapamil

Finally, we investigated gene knockdowns in response to verapamil treatment. Unlike in eukaryotic cells, the calcium channel blocker verapamil does not affect Ca^{2+} levels in *E. coli*.[60] Instead, it induces membrane depolarization and activates the extra-cytoplasmic RpoE response via DegP and PspA, independently of the envelope stress response system CpxR.[61] Although the exact molecular mechanism of verapamil remains unclear, CRISPRi screening revealed that the following systems were affected: intermembrane phospholipid transport (*mlaCDE*), the Tol-Pal system (*tolAQR* and *pal*), the Sec protein translocation system (*secF* and *yajC*), and the twin-arginine protein translocation (Tat) system (*tatAC*) (Figure 3F). However, a *yajC* null mutant, despite being part of the Sec translocon with an unknown function, exhibited similar verapamil-induced growth retardation as the wild-type (Figure S6A). Notably, growth profiles showed increasing variability between replicated cultures over time, particularly after 4 h when a diauxic growth pattern emerged (Figure S6G). This suggests that complete *yajC* deletion may accelerate resistance development. Further investigation is needed to elucidate the precise mechanism of verapamil and its potential interactions with the Sec translocon.

In conclusion, the genome-scale CRISPRi screening provides a valuable dataset that captures the diverse cellular processes involved in antibiotic responses in *E. coli*. Importantly, it reveals the fitness effects of essential genes by modulating their expression levels without causing complete gene disruption.

Responses to DNA damaging agents: MMS, phleomycin, mitomycin C, and novobiocin

Next, we investigated the responses of essential genes to DNA-damaging antibiotics, including MMS, phleomycin, mitomycin C, and novobiocin (Figures 4A and S7). Two genes, *rpoS* and *yacG*, were found to be significantly more essential under DNA-damaging conditions (Figures 4A and 4B). The stress response sigma factor RpoS, a key effector of DNA-related stress, showed an average decrease in ER by 2.0-fold when exposed to DNA-damaging agents. In contrast, the ER of sgRNAs targeting *rpoS* in LB media was 1.98, indicating a preference for silencing *rpoS* under stress-free conditions. This finding aligns with the known role of RpoS in mediating DNA repair by inducing a network of stress-response genes.[62]

The population of sgRNAs targeting the endogenous gyrase inhibitor gene *yacG* was depleted by an average of 1.9-fold when exposed to the four DNA-damaging agents (Figures 4A

and 4B). Despite the potential antibiotic tolerance conferred by YacG, its increased essentiality under novobiocin treatment was unexpected. Both YacG and novobiocin are gyrase inhibitors, so one might anticipate a synergistic effect. However, the opposite was observed. This discrepancy can be explained by their differing molecular mechanisms: the gyrase complex induces negative supercoiling of double-stranded DNA by exchanging strands after double-strand breaks.[63] Novobiocin stalls gyrase by inhibiting the ATPase activity of GyrB, leading to double-strand breaks, while YacG prevents the gyrase complex from binding to DNA,[17] thus mitigating the damage caused by novobiocin. This protective effect of YacG also appeared to be beneficial against the other three DNA-damaging agents.

Four additional genes—*degP*, *ybbC*, *yqcG*, and *yciE*—were significantly affected by CRISPRi knockdowns under three DNA-damaging agents, although their functions are not well characterized (Figure 4A).

Notably, glutamate racemase (MurI) showed a significant change in ER in response to phleomycin and mitomycin C (Figures 4A and 4B). Additionally, genes involved in peptidoglycan biosynthesis (*mur* genes, including *murC*) exhibited more than a 1.5-fold change in ERs, although they did not meet the mean ER criterion (>0.25) due to low ERs in LB conditions (Figure 4C; Table S2). Interestingly, MurI exhibits gyrase inhibitory activity when activated by UDP-N-acetylmuramyl-L-alanine,[64] a product of UDP-N-acetylmuramate-L-alanine ligase (MurC). Although the exact mechanism of gyrase inhibition by MurI is unknown, it may be similar to YacG in protecting against DNA damage, as evidenced by the decreased ERs of *murI*, *murC*, and *yacG* under DNA-damaging conditions (Figures 4B and 4C).

Several peptidoglycan biosynthetic genes are encoded in the *ftsLI-murEF-mraY-murD-ftsW-murGC* operon. The leader gene *ftsL*, which encodes an essential component for cell division protein assembly and recruitment, showed a 1.8-fold decrease in ER, though it did not meet the average ER > 0.25 criterion (Figures 4C and 4D). The molecular mechanism by which FtsL protects against DNA damage is unclear, but the connection between DNA damage and cell wall synthesis may be crucial for coordinating DNA replication and cell division. Alternatively, CRISPRi targeting of *ftsL* may have a polar effect on the operon, altering fitness through *murC*, even though *ftsL* itself does not appear to directly protect against DNA damage (Figure 4D). Although not all DNA repair systems in *E. coli* exhibited significant ER changes, the homology-directed repair genes *recO* and *recA* showed decreased ERs in response to mitomycin C and MMS. Knockout of *recO* resulted in increased sensitivity to these antibiotics (Figures 4E and S8), while no significant changes were observed for phleomycin and novobiocin. This is likely because *recA* and *recO* provide protection against DNA crosslinking and methylation induced by mitomycin C and MMS, respectively, but do not play a major role in repairing the double-strand breaks caused by phleomycin and novobiocin.

Responses to translation inhibitors: Erythromycin and puromycin

When translation inhibitors erythromycin and puromycin were used, only a few genes showed significant responses. Notably, the ERs of the proteases, DegP and Lon, which are involved in protein quality control,[12,65] were significantly altered (Figures 5A and S9). The ERs of *degP* decreased in the presence of these antibiotics compared to those in LB, highlighting its critical role under translational stress. Conversely, *lon* knockdown had a beneficial effect under translational stress, according to the CRISPRi screening (Figure 5A). This is because Lon protease destabilizes the multidrug efflux pump AcrAB-TolC,[66] which is the most versatile efflux system against antibiotics (Figure 2D). Consistently, *lon* knockout strain exhibited insensitivity to erythromycin and puromycin (Figure S10). Therefore, these findings suggest that in the presence of antibiotics, stabilization of the efflux system through *lon* inhibition outweighs the benefits of its role in protein quality control. Additionally, UDP-3-*O*-acyl-N-acetylglucosamine deacetylase (LpxC), involved in lipid A biosynthesis, was crucial for the response to translation inhibitors. This aligns with previous studies showing that LpxC inactivation increases antibiotic permeability and causes leakage of periplasmic enzymes[67,68] (Figure 5A).

Furthermore, auxiliary factors previously reported to be involved in translational stress[69] showed distinct responses to different translation inhibitors (Figure 5B). For instance, knockdown of the ribosome rescue factor ArfA was detrimental when cells were treated with puromycin, with ER decreasing by 17.5%. ArfA protects against puromycin by releasing puromycylated peptides from stalled ribosomes. However, ArfA had no beneficial effect during erythromycin treatment, with its ER increasing by 9.5%. This difference can be explained by the fact that erythromycin inhibits aminoacyl transfer from the A-site to the P-site, preventing ArfA from accessing the aminoacyl-occupied A-site for rescue. These findings illustrate the complexity of *E. coli*'s response to antibiotic stresses induced by different molecular mechanisms, highlighting the distinct roles of various proteases and auxiliary factors in mediating antibiotic resistance.

DISCUSSION

This study demonstrates the efficacy of a genome-wide CRISPRi approach for screening essential genes and assessing gene fitness under various antibiotic treatments. Compared to conventional knockout methods, CRISPRi significantly reduces the time and effort required to screen the entire coding sequence. Once the library is constructed, gRNA populations can be efficiently monitored against diverse stresses through simple cell culture, plasmid extraction, and high-throughput sequencing. Notably, there was substantial agreement between essential genes identified in a previous knockout study[1] and those identified through CRISPRi screening, highlighting the capability of CRISPRi to rapidly identify essential genes under specific conditions.

Our application of CRISPRi screening uncovered genetic responses of *E. coli* to various antibiotics, revealing universal stress responses. For instance, periplasmic protease DegP, involved in protein quality control and membrane barrier reinforcement, exhibited a protective role across multiple antibiotics. Moreover, inhibition of the uncharacterized gate family protein YjiG proved beneficial against antibiotics treatment, suggesting its potential involvement in antibiotic entry, as supported by

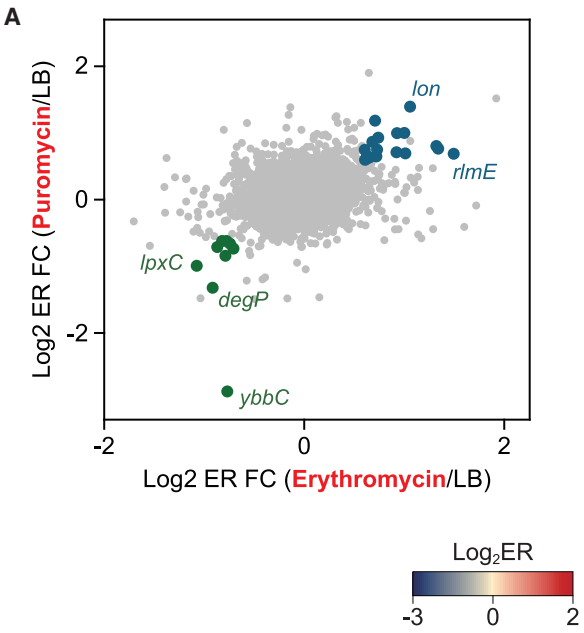

Figure 5. Genetic responses involved in translational stress

(A) The ER changes of genes under erythromycin and puromycin treatment.

(B) Heatmap showing the ER values of genes required for translational stress responses.[69] See also Figures S9, S10, Tables S2, and S4.

growth profiling of knockout strains (Figure 2). Various efflux pumps, including the outer membrane channel TolC and its associated partners, showed fitness changes when inhibited by CRISPRi. Targeting *tolC* with sgRNA led to cell extinction under most antibiotic treatments, emphasizing the critical role of TolC in antibiotic efflux. However, the essentiality of other efflux pumps varied based on the type of antibiotic, indicating distinct ligand specificities for each pump.

In addition to universal responses, CRISPRi exposed biological processes involved in specific antibiotic treatments. Over a thousand genes exhibited significant ER changes, indicating the broad spectrum of cellular processes affected by antibiotic action. We identified genes previously unrecognized for their role in antibiotic stress response, such as the Sap transporter responding to multiple antibiotics, including pyocyanin, CCCP, and rifampicin (Figure 3). This underscores the potential of genome-wide CRISPRi screening to identify hidden factors involved in antibiotic responses.

CRISPRi screening also revealed that many essential membranous proteins contribute to antibiotic tolerance. While the *E. coli* membrane and periplasmic proteome have remained under-characterized, likely due to experimental technique limitations, the robustness of CRISPRi screening was evident in its ability to identify membrane proteins, such as the outer membrane beta-barrel assembly machinery (BAM). Furthermore, the non-disruptive nature of CRISPRi allowed for screening of essential genes that cannot be probed by gene disruption, such as the sigma 70 factor (RpoD) alongside BAM complex.

Moreover, CRISPRi screening identified not only genes required for antibiotic tolerance but also genes whose inactivation enhances survival. For example, glutathione biosynthetic genes—glutamate-cysteine ligase (*gshA*), glutathione synthetase (*gshB*), and glutathionylspermidine synthetase (*gss*)—were found to be detrimental because glutathione can serve as a source of reactive oxygen species in the presence of pyocyanin. Additionally, we identified the Sap transporter, which conferred resistance to multiple antibiotics (Figure 3). This expands the known role of *sapF*, suggesting it may also function as an entry route for certain antibiotics, beyond its involvement in antimicrobial peptide susceptibility. This observation warrants further exploration into how the Sap system might influence antibiotic uptake and resistance. This dataset sheds light on potential bacterial resistance mechanisms to various antibiotics and uncovers genetic factors that could serve as targets for therapeutic interventions.

In conclusion, genome-wide CRISPRi screening provides a rapid and robust method for exploring fundamental processes in *E. coli*. This study yields insights into the molecular mechanisms underlying antibiotic responses and the genetic basis. The screening results constitute a valuable dataset for identifying potential targets for antibiotics or sensitizers and generating hypotheses for further studies to elucidate transcriptional regulatory networks and resistance mechanisms with potential clinical relevance.

Limitations of the study

A limitation of the CRISPRi approach is its focus on transcriptional inhibition, precluding the induction of silent genes under antibiotics challenge. This can be addressed by employing CRISPR activation (CRISPRa), utilizing dCas9 fused with transcriptional activators for targeted gene activation.[70] Recent advancements in dCas9 engineering have overcome restrictions related to the protospacer adjacent motif (PAM) sequence and stringent CRISPRa target requirements, improving predictive rules for designing effective gRNAs.[71] Integrating CRISPRa could complement the limitations of CRISPRi screening, and investigating gene activation in *E. coli* under antibiotic stress represents a promising direction for future research.

RESOURCE AVAILABILITY

Lead contact

Requests for further information and resources should be directed to and will be fulfilled by the lead contact, Suhyung Cho (shcho95@kaist.ac.kr).

Materials availability

Reagents generated in this study are available from the lead contact with Materials Transfer Agreements.

Data and code availability

- Original data of CRISPRi amplicon sequencing have been deposited at European Nucleotide Archive as ENA: PRJEB33267 (https://www.ebi.ac.uk/ena/browser/view/PRJEB33267) and are publicly available as of the date of publication.
- All original codes are available in this paper's supplemental information.
- Any additional information required to reanalyze the data reported in this paper is available from the lead contact upon request.

ACKNOWLEDGMENTS

This work was supported by the National Research Foundation of Korea (NRF) (grants 2021R1A2C1012589 to S.C. and 2021M3A9I4024308 to B.-K.C.) funded by the Ministry of Science and ICT, Republic of Korea, the Basic Science Research Program through NRF funded by the Ministry of Education (RS-2023-00246928 to S.C.), the Novo Nordisk Foundation (grant NNF20CC0035580 to B.O.P.), and the Y.C. Fung Endowed Chair in Bioengineering at UC San Diego (to B.O.P.).

AUTHOR CONTRIBUTIONS

B.-K.C. and S.C. conceived and supervised the study. D.C., B.-K.C., and S.C. designed the experiments. D.C., E.L., K.K., S.H., and S.C. performed the experiments. D.C., B.O.P., B.-K.C., and S.C. analyzed the data. D.C., K.J.J., B. O.P., B.-K.C., and S.C. wrote the manuscript.

DECLARATION OF INTERESTS

The authors declare no competing interests.

STAR★METHODS

Detailed methods are provided in the online version of this paper and include the following:

- KEY RESOURCES TABLE
- METHOD DETAILS
  - Bacterial strains
  - Individual sgRNA plasmids construction
  - Microscopy
  - Design of sgRNA library
  - sgRNA library construction
  - Generation of antibiotics treated populations
  - sgRNA library sequencing
  - Measuring fitness effect of knockout strains
- QUANTIFICATION AND STATISTICAL ANALYSIS
  - Quantification of gene fitness
  - Statistical analysis

SUPPLEMENTAL INFORMATION

Supplemental information can be found online at https://doi.org/10.1016/j.isci.2025.112435.

Received: September 23, 2024
Revised: February 6, 2025
Accepted: April 10, 2025
Published: April 15, 2025

REFERENCES

1. Baba, T., Ara, T., Hasegawa, M., Takai, Y., Okumura, Y., Baba, M., Datsenko, K.A., Tomita, M., Wanner, B.L., and Mori, H. (2006). Construction of *Escherichia coli* K-12 in-frame, single-gene knockout mutants: the Keio collection. Mol. Syst. Biol. *2*, 2006.0008. https://doi.org/10.1038/msb4100050.
2. Choe, D., Kim, U., Hwang, S., Seo, S.W., Kim, D., Cho, S., Palsson, B., and Cho, B.K. (2023). Revealing Causes for False-Positive and False-Negative Calling of Gene Essentiality in *Escherichia coli* Using Transposon Insertion Sequencing. mSystems *8*, e0089622. https://doi.org/10.1128/msystems.00896-22.
3. Gilbert, L.A., Horlbeck, M.A., Adamson, B., Villalta, J.E., Chen, Y., Whitehead, E.H., Guimaraes, C., Panning, B., Ploegh, H.L., Bassik, M.C., et al. (2014). Genome-Scale CRISPR-Mediated Control of Gene Repression and Activation. Cell *159*, 647–661. https://doi.org/10.1016/j.cell.2014.09.029.
4. Qi, L.S., Larson, M.H., Gilbert, L.A., Doudna, J.A., Weissman, J.S., Arkin, A.P., and Lim, W.A. (2013). Repurposing CRISPR as an RNA-guided platform for sequence-specific control of gene expression. Cell *152*, 1173–1183. https://doi.org/10.1016/j.cell.2013.02.022.
5. Peters, J.M., Colavin, A., Shi, H., Czarny, T.L., Larson, M.H., Wong, S., Hawkins, J.S., Lu, C.H.S., Koo, B.M., Marta, E., et al. (2016). A Comprehensive, CRISPR-based Functional Analysis of Essential Genes in Bacteria. Cell *165*, 1493–1506. https://doi.org/10.1016/j.cell.2016.05.003.
6. Shin, J., Bae, J., Lee, H., Kang, S., Jin, S., Song, Y., Cho, S., and Cho, B.K. (2023). Genome-wide CRISPRi screen identifies enhanced autolithotrophic phenotypes in acetogenic bacterium *Eubacterium limosum*. Proc. Natl. Acad. Sci. USA *120*, e2216244120. https://doi.org/10.1073/pnas.2216244120.
7. Evers, B., Jastrzebski, K., Heijmans, J.P.M., Grernrum, W., Beijersbergen, R.L., and Bernards, R. (2016). CRISPR knockout screening outperforms shRNA and CRISPRi in identifying essential genes. Nat. Biotechnol. *34*, 631–633. https://doi.org/10.1038/nbt.3536.
8. Wang, T., Guan, C., Guo, J., Liu, B., Wu, Y., Xie, Z., Zhang, C., and Xing, X. H. (2018). Pooled CRISPR interference screening enables genome-scale functional genomics study in bacteria with superior performance. Nat. Commun. *9*, 2475. https://doi.org/10.1038/s41467-018-04899-x.
9. Choe, D., Szubin, R., Dahesh, S., Cho, S., Nizet, V., Palsson, B., and Cho, B.K. (2018). Genome-scale analysis of Methicillin-resistant *Staphylococcus aureus* USA300 reveals a tradeoff between pathogenesis and drug resistance. Sci. Rep. *8*, 2215. https://doi.org/10.1038/s41598-018-20661-1.
10. Cho, S., Choe, D., Lee, E., Kim, S.C., Palsson, B., and Cho, B.K. (2018). High-Level dCas9 Expression Induces Abnormal Cell Morphology in *Escherichia coli*. ACS Synth. Biol. *7*, 1085–1094. https://doi.org/10.1021/acssynbio.7b00462.
11. Zhu, X., Luo, H., Yu, X., Lv, H., Su, L., Zhang, K., and Wu, J. (2024). Genome-Wide CRISPRi Screening of Key Genes for Recombinant Protein Expression in *Bacillus Subtilis*. Adv. Sci. *11*, e2404313. https://doi.org/10.1002/advs.202404313.
12. Laskowska, E., Kuczyńska-Wiśnik, D., Skórko-Glonek, J., and Taylor, A. (1996). Degradation by proteases Lon, Clp and HtrA, of *Escherichia coli* proteins aggregated *in vivo* by heat shock; HtrA protease action *in vivo* and *in vitro*. Mol. Microbiol. *22*, 555–571. https://doi.org/10.1046/j.1365-2958.1996.1231493.x.
13. Skorko-Glonek, J., Zurawa, D., Kuczwara, E., Wozniak, M., Wypych, Z., and Lipinska, B. (1999). The *Escherichia coli* heat shock protease HtrA participates in defense against oxidative stress. Mol. Gen. Genet. *262*, 342–350. https://doi.org/10.1007/s004380051092.
14. Strauch, K.L., and Beckwith, J. (1988). An *Escherichia coli* mutation preventing degradation of abnormal periplasmic proteins. Proc. Natl. Acad. Sci. USA *85*, 1576–1580. https://doi.org/10.1073/pnas.85.5.1576.
15. Waller, P.R., and Sauer, R.T. (1996). Characterization of *degQ* and *degS*, *Escherichia coli* genes encoding homologs of the DegP protease. J. Bacteriol. *178*, 1146–1153. https://doi.org/10.1128/jb.178.4.1146-1153.1996.
16. Meltzer, M., Hasenbein, S., Mamant, N., Merdanovic, M., Poepsel, S., Hauske, P., Kaiser, M., Huber, R., Krojer, T., Clausen, T., and Ehrmann, M. (2009). Structure, function and regulation of the conserved serine

proteases DegP and DegS of *Escherichia coli*. Res. Microbiol. *160*, 660–666. https://doi.org/10.1016/j.resmic.2009.07.012.

17. Sengupta, S., and Nagaraja, V. (2008). YacG from *Escherichia coli* is a specific endogenous inhibitor of DNA gyrase. Nucleic Acids Res. *36*, 4310–4316. https://doi.org/10.1093/nar/gkn355.
18. Daley, D.O., Rapp, M., Granseth, E., Melén, K., Drew, D., and von Heijne, G. (2005). Global topology analysis of the *Escherichia coli* inner membrane proteome. Science *308*, 1321–1323. https://doi.org/10.1126/science.1109730.
19. Loewen, S.K., Ng, A.M., Yao, S.Y., Cass, C.E., Baldwin, S.A., and Young, J.D. (1999). Identification of amino acid residues responsible for the pyrimidine and purine nucleoside specificities of human concentrative Na(+) nucleoside cotransporters hCNT1 and hCNT2. J. Biol. Chem. *274*, 24475–24484. https://doi.org/10.1074/jbc.274.35.24475.
20. Hantke, K. (2003). Is the bacterial ferrous iron transporter FeoB a living fossil? Trends Microbiol. *11*, 192–195. https://doi.org/10.1016/s0966-842x(03)00100-8.
21. Caldas, T., Binet, E., Bouloc, P., and Richarme, G. (2000). Translational defects of *Escherichia coli* mutants deficient in the Um(2552) 23S ribosomal RNA methyltransferase RrmJ/FTSJ. Biochem. Biophys. Res. Commun. *271*, 714–718. https://doi.org/10.1006/bbrc.2000.2702.
22. Toh, S.M., and Mankin, A.S. (2008). An indigenous posttranscriptional modification in the ribosomal peptidyl transferase center confers resistance to an array of protein synthesis inhibitors. J. Mol. Biol. *380*, 593–597. https://doi.org/10.1016/j.jmb.2008.05.027.
23. Babosan, A., Fruchard, L., Krin, E., Carvalho, A., Mazel, D., and Baharoglu, Z. (2022). Nonessential tRNA and rRNA modifications impact the bacterial response to sub-MIC antibiotic stress. Microlife *3*, uqac019. https://doi.org/10.1093/femsml/uqac019.
24. Anes, J., McCusker, M.P., Fanning, S., and Martins, M. (2015). The ins and outs of RND efflux pumps in *Escherichia coli*. Front. Microbiol. *6*, 587. https://doi.org/10.3389/fmicb.2015.00587.
25. Du, D., Wang-Kan, X., Neuberger, A., van Veen, H.W., Pos, K.M., Piddock, L.J.V., and Luisi, B.F. (2018). Multidrug efflux pumps: structure, function and regulation. Nat. Rev. Microbiol. *16*, 523–539. https://doi.org/10.1038/s41579-018-0048-6.
26. Dhamdhere, G., and Zgurskaya, H.I. (2010). Metabolic shutdown in *Escherichia coli* cells lacking the outer membrane channel TolC. Mol. Microbiol. *77*, 743–754. https://doi.org/10.1111/j.1365-2958.2010.07245.x.
27. Vega, D.E., and Young, K.D. (2014). Accumulation of periplasmic enterobactin impairs the growth and morphology of *Escherichia coli tolC* mutants. Mol. Microbiol. *91*, 508–521. https://doi.org/10.1111/mmi.12473.
28. Neuberger, A., Du, D., and Luisi, B.F. (2018). Structure and mechanism of bacterial tripartite efflux pumps. Res. Microbiol. *169*, 401–413. https://doi.org/10.1016/j.resmic.2018.05.003.
29. Nishino, K., and Yamaguchi, A. (2001). Analysis of a complete library of putative drug transporter genes in *Escherichia coli*. J. Bacteriol. *183*, 5803–5812. https://doi.org/10.1128/JB.183.20.5803-5812.2001.
30. Tikhonova, E.B., Wang, Q., and Zgurskaya, H.I. (2002). Chimeric analysis of the multicomponent multidrug efflux transporters from gram-negative bacteria. J. Bacteriol. *184*, 6499–6507. https://doi.org/10.1128/JB.184.23.6499-6507.2002.
31. Elkins, C.A., and Nikaido, H. (2002). Substrate specificity of the RND-type multidrug efflux pumps AcrB and AcrD of *Escherichia coli* is determined predominantly by two large periplasmic loops. J. Bacteriol. *184*, 6490–6498. https://doi.org/10.1128/JB.184.23.6490-6499.2002.
32. Ma, D., Cook, D.N., Alberti, M., Pon, N.G., Nikaido, H., and Hearst, J.E. (1993). Molecular cloning and characterization of *acrA* and *acrE* genes of *Escherichia coli*. J. Bacteriol. *175*, 6299–6313. https://doi.org/10.1128/jb.175.19.6299-6313.1993.
33. Hassan, H.M., and Fridovich, I. (1980). Mechanism of the antibiotic action pyocyanine. J. Bacteriol. *141*, 156–163. https://doi.org/10.1128/jb.141.1.156-163.1980.
34. Muller, M. (2002). Pyocyanin induces oxidative stress in human endothelial cells and modulates the glutathione redox cycle. Free Radic. Biol. Med. *33*, 1527–1533. https://doi.org/10.1016/s0891-5849(02)01087-0.
35. Ran, H., Hassett, D.J., and Lau, G.W. (2003). Human targets of *Pseudomonas aeruginosa* pyocyanin. Proc. Natl. Acad. Sci. USA *100*, 14315–14320. https://doi.org/10.1073/pnas.2332354100.
36. Britton, L., and Fridovich, I. (1977). Intracellular localization of the superoxide dismutases of *Escherichia coli*: a reevaluation. J. Bacteriol. *131*, 815–820. https://doi.org/10.1128/jb.131.3.815-820.1977.
37. Amabile-Cuevas, C.F., and Demple, B. (1991). Molecular characterization of the *soxRS* genes of *Escherichia coli*: two genes control a superoxide stress regulon. Nucleic Acids Rese. *19*, 4479–4484. https://doi.org/10.1093/nar/19.16.4479.
38. Loui, C., Chang, A.C., and Lu, S. (2009). Role of the ArcAB two-component system in the resistance of *Escherichia coli* to reactive oxygen stress. BMC Microbiol. *9*, 183. https://doi.org/10.1186/1471-2180-9-183.
39. Lee, J.H., Yeo, W.S., and Roe, J.H. (2004). Induction of the *sufA* operon encoding Fe-S assembly proteins by superoxide generators and hydrogen peroxide: involvement of OxyR, IHF and an unidentified oxidant-responsive factor. Mol. Microbiol. *51*, 1745–1755. https://doi.org/10.1111/j.1365-2958.2003.03946.x.
40. Yang, W., Rogers, P.A., and Ding, H. (2002). Repair of nitric oxide-modified ferredoxin [2Fe-2S] cluster by cysteine desulfurase (IscS). J. Biol. Chem. *277*, 12868–12873. https://doi.org/10.1074/jbc.M109485200.
41. Soballe, B., and Poole, R.K. (1999). Microbial ubiquinones: multiple roles in respiration, gene regulation and oxidative stress management. Microbiology (Read.) *145*, 1817–1830. https://doi.org/10.1099/13500872-145-8-1817.
42. O'Malley, Y.Q., Reszka, K.J., Spitz, D.R., Denning, G.M., and Britigan, B.E. (2004). *Pseudomonas aeruginos*a pyocyanin directly oxidizes glutathione and decreases its levels in airway epithelial cells. Am. J. Physiol. Lung Cell. Mol. Physiol. *287*, L94–L103. https://doi.org/10.1152/ajplung.00025.2004.
43. Feng, Z., Liu, D., Wang, L., Wang, Y., Zang, Z., Liu, Z., Song, B., Gu, L., Fan, Z., Yang, S., et al. (2020). A Putative Efflux Transporter of the ABC Family, YbhFSR, in *Escherichia coli* Functions in Tetracycline Efflux and Na(+)(Li(+))/H(+) Transport. Front. Microbiol. *11*, 556. https://doi.org/10.3389/fmicb.2020.00556.
44. Yamanaka, Y., Shimada, T., Yamamoto, K., and Ishihama, A. (2016). Transcription factor CecR (YbiH) regulates a set of genes affecting the sensitivity of *Escherichia coli* against cefoperazone and chloramphenicol. Microbiology *162*, 1253–1264. https://doi.org/10.1099/mic.0.000292.
45. Yoshida, Y., Sugiyama, S., Oyamada, T., Yokoyama, K., and Makino, K. (2012). Novel members of the phosphate regulon in *Escherichia coli* O157:H7 identified using a whole-genome shotgun approach. Gene *502*, 27–35. https://doi.org/10.1016/j.gene.2012.03.064.
46. Prossliner, T., Gerdes, K., Sørensen, M.A., and Winther, K.S. (2021). Hibernation factors directly block ribonucleases from entering the ribosome in response to starvation. Nucleic Acids Res. *49*, 2226–2239. https://doi.org/10.1093/nar/gkab017.
47. Sugiyama, Y., Nakamura, A., Matsumoto, M., Kanbe, A., Sakanaka, M., Higashi, K., Igarashi, K., Katayama, T., Suzuki, H., and Kurihara, S. (2016). A Novel Putrescine Exporter SapBCDF of *Escherichia coli*. J. Biol. Chem. *291*, 26343–26351. https://doi.org/10.1074/jbc.M116.762450.
48. Parra-Lopez, C., Baer, M.T., and Groisman, E.A. (1993). Molecular genetic analysis of a locus required for resistance to antimicrobial peptides in *Salmonella typhimurium*. EMBO J. *12*, 4053–4062. https://doi.org/10.1002/j.1460-2075.1993.tb06089.x.
49. Shelton, C.L., Raffel, F.K., Beatty, W.L., Johnson, S.M., and Mason, K.M. (2011). Sap transporter mediated import and subsequent degradation of antimicrobial peptides in *Haemophilus*. PLoS Pathog. *7*, e1002360. https://doi.org/10.1371/journal.ppat.1002360.

50. Velkov, T., Thompson, P.E., Nation, R.L., and Li, J. (2010). Structure–activity relationships of polymyxin antibiotics. J. Med. Chem. *53*, 1898–1916. https://doi.org/10.1021/jm900999h.

51. Silva, K.E.D., Rossato, L., Leite, A.F., and Simionatto, S. (2022). Overview of polymyxin resistance in *Enterobacteriaceae*. Rev. Soc. Bras. Med. Trop. *55*, e0349. https://doi.org/10.1590/0037-8682-0349-2021.

52. Winfield, M.D., and Groisman, E.A. (2004). Phenotypic differences between *Salmonella* and *Escherichia coli* resulting from the disparate regulation of homologous genes. Proc. Natl. Acad. Sci. USA *101*, 17162–17167. https://doi.org/10.1073/pnas.0406038101.

53. Zhou, Z., Lin, S., Cotter, R.J., and Raetz, C.R. (1999). Lipid A modifications characteristic of *Salmonella typhimurium* are induced by NH4VO3 in *Escherichia coli* K12. Detection of 4-amino-4-deoxy-L-arabinose, phosphoethanolamine and palmitate. J. Biol. Chem. *274*, 18503–18514. https://doi.org/10.1074/jbc.274.26.18503.

54. Bertani, B., and Ruiz, N. (2018). Function and Biogenesis of Lipopolysaccharides. EcoSal Plus *8*. https://doi.org/10.1128/ecosalplus.ESP-0001-2018.

55. Manioglu, S., Modaresi, S.M., Ritzmann, N., Thoma, J., Overall, S.A., Harms, A., Upert, G., Luther, A., Barnes, A.B., Obrecht, D., et al. (2022). Antibiotic polymyxin arranges lipopolysaccharide into crystalline structures to solidify the bacterial membrane. Nat. Commun. *13*, 6195. https://doi.org/10.1038/s41467-022-33838-0.

56. Ruiz, N., Wu, T., Kahne, D., and Silhavy, T.J. (2006). Probing the barrier function of the outer membrane with chemical conditionality. ACS Chem. Biol. *1*, 385–395. https://doi.org/10.1021/cb600128v.

57. Wu, T., Malinverni, J., Ruiz, N., Kim, S., Silhavy, T.J., and Kahne, D. (2005). Identification of a multicomponent complex required for outer membrane biogenesis in *Escherichia coli*. Cell *121*, 235–245. https://doi.org/10.1016/j.cell.2005.02.015.

58. Kanehisa, M., Sato, Y., and Kawashima, M. (2022). KEGG mapping tools for uncovering hidden features in biological data. Protein Sci. *31*, 47–53. https://doi.org/10.1002/pro.4172.

59. Roland, S., Ferone, R., Harvey, R.J., Styles, V.L., and Morrison, R.W. (1979). The characteristics and significance of sulfonamides as substrates for *Escherichia coli* dihydropteroate synthase. J. Biol. Chem. *254*, 10337–10345.

60. Holland, I.B., Jones, H.E., Campbell, A.K., and Jacq, A. (1999). An assessment of the role of intracellular free Ca2+ in *E. coli*. Biochimie *81*, 901–907. https://doi.org/10.1016/s0300-9084(99)00205-9.

61. Andersen, C.L., Holland, I.B., and Jacq, A. (2006). Verapamil, a Ca2+ channel inhibitor acts as a local anesthetic and induces the sigma E dependent extra-cytoplasmic stress response in *E. coli*. Biochim. Biophys. Acta *1758*, 1587–1595. https://doi.org/10.1016/j.bbamem.2006.05.022.

62. Al Mamun, A.A.M., Lombardo, M.J., Shee, C., Lisewski, A.M., Gonzalez, C., Lin, D., Nehring, R.B., Saint-Ruf, C., Gibson, J.L., Frisch, R.L., et al. (2012). Identity and function of a large gene network underlying mutagenic repair of DNA breaks. Science *338*, 1344–1348. https://doi.org/10.1126/science.1226683.

63. Williams, N.L., and Maxwell, A. (1999). Probing the two-gate mechanism of DNA gyrase using cysteine cross-linking. Biochemistry *38*, 13502–13511. https://doi.org/10.1021/bi9912488.

64. Ashiuchi, M., Kuwana, E., Yamamoto, T., Komatsu, K., Soda, K., and Misono, H. (2002). Glutamate racemase is an endogenous DNA gyrase inhibitor. J. Biol. Chem. *277*, 39070–39073. https://doi.org/10.1074/jbc.C200253200.

65. Zhang, S., Cheng, Y., Ma, J., Wang, Y., Chang, Z., and Fu, X. (2019). DegP degrades a wide range of substrate proteins in *Escherichia coli* under stress conditions. Biochem. J. *476*, 3549–3564. https://doi.org/10.1042/BCJ20190446.

66. Nicoloff, H., and Andersson, D.I. (2013). Lon protease inactivation, or translocation of the *lon* gene, potentiate bacterial evolution to antibiotic resistance. Mol. Microbiol. *90*, 1233–1248. https://doi.org/10.1111/mmi.12429.

67. Normark, S. (1970). Genetics of a chain-forming mutant of *Escherichia coli*. Transduction and dominance of the *envA* gene mediating increased penetration to some antibacterial agents. Genet. Res. *16*, 63–78. https://doi.org/10.1017/s0016672300002287.

68. Young, K., and Silver, L.L. (1991). Leakage of periplasmic enzymes from *envA1* strains of *Escherichia coli*. J. Bacteriol. *173*, 3609–3614. https://doi.org/10.1128/jb.173.12.3609-3614.1991.

69. Starosta, A.L., Lassak, J., Jung, K., and Wilson, D.N. (2014). The bacterial translation stress response. FEMS Microbiol. Rev. *38*, 1172–1201. https://doi.org/10.1111/1574-6976.12083.

70. Dong, C., Fontana, J., Patel, A., Car, J.M., and Zalatan, J.G. (2018). Synthetic CRISPR-Cas gene activators for transcriptional reprogramming in bacteria. Nat. Commun. *9*, 2489. https://doi.org/10.1038/s41467-018-04901-6.

71. Fontana, J., Dong, C., Kiattisewee, C., Chavali, V.P., Tickman, B.I., Car, J.M., and Zalatan, J.G. (2020). Effective CRISPRa-mediated control of gene expression in bacteria must overcome strict target site requirements. Nat. Commun. *11*, 1618. https://doi.org/10.1038/s41467-020-15454-y.

72. Datsenko, K.A., and Wanner, B.L. (2000). One-step inactivation of chromosomal genes in *Escherichia coli* K-12 using PCR products. Proc. Natl. Acad. Sci. USA *97*, 6640–6645. https://doi.org/10.1073/pnas.120163297.

73. Bikard, D., Jiang, W., Samai, P., Hochschild, A., Zhang, F., and Marraffini, L.A. (2013). Programmable repression and activation of bacterial gene expression using an engineered CRISPR-Cas system. Nucleic Acids Res. *41*, 7429–7437. https://doi.org/10.1093/nar/gkt520.

74. Sanjana, N.E., Shalem, O., and Zhang, F. (2014). Improved vectors and genome-wide libraries for CRISPR screening. Nat. Methods *11*, 783–784. https://doi.org/10.1038/nmeth.3047.

75. Shalem, O., Sanjana, N.E., Hartenian, E., Shi, X., Scott, D.A., Mikkelson, T., Heckl, D., Ebert, B.L., Root, D.E., Doench, J.G., and Zhang, F. (2014). Genome-scale CRISPR-Cas9 knockout screening in human cells. Science *343*, 84–87. https://doi.org/10.1126/science.1247005.

STAR★METHODS

KEY RESOURCES TABLE

REAGENT or RESOURCE	SOURCE	IDENTIFIER
Bacterial and virus strains		
E. coli K-12 MG1655 *mrfp-npt*II	This study	N/A
E. coli Endura ElectroCompetent Cells	LGC Biosearch technologies	Cat. No. 60242-1
The KEIO strain collection	Horizon Discovery	Cat. No. OEC4988
Chemicals, peptides, and recombinant proteins		
LB Miller broth	BD Difco	244620
Carbonyl Cyanide m-Chlorophenylhydrazone (CCCP)	Sigma-Aldrich	C2759
Polymyxin B	Sigma-Aldrich	P1004
Pyocyanin	Sigma-Aldrich	P0046
Rifampicin	Sigma-Aldrich	R3501
Sulfamethizole	Sigma-Aldrich	S5632
Verapamil	Sigma-Aldrich	V4629
Puromycin	Sigma-Aldrich	P7255
Erythromycin	Sigma-Aldrich	E5389
Phleomycin	Sigma-Aldrich	P9564
Mitomycin C	Sigma-Aldrich	M0503
MMS	Sigma-Aldrich	129925
Novobiocin	Sigma-Aldrich	N1628
Deposited data		
All amplicon sequencing data	This study	European Nucleotide Archive (ENA): PRJEB33267
Oligonucleotides		
See Table S5 for oligonucleotides used in this study.	This study	N/A
See Table S6 for oligonucleotide pool used in this study.	This study	N/A
Recombinant DNA		
pdCas9	Bikard et al.[72]	Addgene 46569
pgRNA-bacteria	Qi et al.[4]	Addgene 44251
Software and algorithms		
CLC Genomics Workbench	CLC Bio	v6.5.1
Python	Python Software Foundation	v3.4.10
In house python scripts for sgRNA design	This study	Datas S1, S2, and S3
Microsoft Excel for Microsoft 365	Microsoft	V2401
Other		
BioTek Synergy H1 Microplate Reader	Agilent	https://www.agilent.com/en/product/microplate-instrumentation/microplate-readers/multimode-microplate-readers/biotek-synergy-h1-multimode-reader-1623193
Eclipse Ti-U Optical Microscope	Nikon	https://www.microscope.healthcare.nikon.com/products/inverted-microscopes/eclipse-ti-series

METHOD DETAILS

Bacterial strains

To test the CRISPRi system, an *mrfp-nptII* (neomycin phosphotransferase; kanamycin resistance gene) cassette was introduced into *E. coli* K-12 MG1655 chromosomal DNA between *lacI* and *lacZ* via lambda recombination.[10,72] dCas9 and sgRNA were expressed with separate plasmids, pdCas9 plasmid[73] (cat. #46569; Addgene, Cambridge, MA, USA) and pgRNA-bacteria plasmid[4] (cat. #44251; Addgene) targeting *mrfp* (Figure S1A). *E. coli* cells for sgRNA library construction and for CRISPRi screening were each cultivated in LB medium supplemented with 100 μg/ml ampicillin and 35 μg/ml chloramphenicol plus 100 μg/ml ampicillin, respectively. Single knockout strains were obtained from the KEIO strain collection.[1] The parental strain of the KEIO collection, *E. coli* BW25113, was used as a wild-type control. Growth profiles were monitored on microtiter plates using a Synergy H1 microplate reader (Agilent, Santa Clara, CA, USA). The primer sequences were summarized in Table S5.

Individual sgRNA plasmids construction

To construct the sgRNA plasmids for *groS*, *pfkB*, *rpoD*, *rpoS*, and *mrfp*, sgRNAs were designed for the non-template strands of the target genes within 100 nt of the start codon of each gene, except for *mrfp*. The cloned inserts were PCR amplified using a forward primer with a *Spe*I restriction enzyme site (5′-GTCAACTAGTA-spacer-GTTTTAGAGCTAGAAATAGCAAGTT) and a reverse primer with a *Hind*III restriction enzyme site (5′-TTTGTTCGGGCCCAAGCTTCA) based on the pgRNA plasmid template. The primer sequences were summarized in Table S5.

Microscopy

To observe the mRFP in *E. coli* K-12 MG1655::*mrfp-nptII*, 5 μl of cell culture was spread on a low melting agarose (1%) pad (1 mm thickness) on a glass slide. After drying for 1–2 min, the pad was covered with a glass coverslip and the cells were observed using a Nikon Eclipse Ti-U Optical Microscope (Nikon, Melville, NY, USA) (Figure S1B).

Design of sgRNA library

All possible sgRNA sequences in the *E. coli* K-12 MG1655 genome were generated and evaluated as previously described.[6] Briefly, candidate sgRNAs were acquired by dissecting all genic regions into 23 mers that began with the protospacer adjacent motif (PAM) sequence. These sequences were subjected to a BLASTN-based search for off-target binding as described previously.[74] Sequences that aligned to more than one locus in the genome were excluded. Then, gRNAs positioned in the CDS were extracted from the CDS list (CDSs extracted from the NC_000913.3 RefSeq annotation) using an in-house Python script (Data S1). Simultaneously, the CDSs were fragmented every 100 nt (Data S2). The first gRNA in a specific CDS fragment was then selected to make the average distance between the gRNAs 100 nt long. If certain CDS fragments contained no gRNA, the last gRNA of the previous fragment was selected (Data S3). Finally, the sequences of the selected gRNAs were extracted. Spacer sequences are listed in Table S6.

sgRNA library construction

The protocol for sgRNA library construction has been modified based on a previous method.[75] As mentioned above, we designed sgRNAs for the CRISPRi system with a ratio of one within 100 nt of all CDSs in *E. coli* K-12 MG1655. A pool of 39,591 oligos consisting of a 20 nt random spacer and additional sequences for the 5′ and 3′ extensions was synthesized in the form of 5′-GCTCAGTCC TAGGTATAATACTAGTA-20 nt spacer-GTTTTAGAGCTAGAAATAGCAAGTTAAAATAAG-3′ by CustomArray Inc. (Bothell, WA, USA) (Table S6). The last base upstream of the spacer sequence was set to "A" to minimize the deviation in transcription activity due to the transcription start nucleotide. The synthetic sgRNA pool was amplified with primers sgRNA_Lib_F and sgRNA_Lib_R (Table S5). The plasmid backbone was amplified from the pgRNA-bacteria plasmid DNA using backbone_F and backbone_R primers and further treated with *Dpn*I to remove the template plasmid. Gel-purified 40 ng insert products (200 bp) and 100 ng vector products (2435 bp) were assembled using a 40 μl reaction and the NEBuilder HiFi DNA Assembly Kit (NEB, Ipswich, MA, USA). Each of the assembled DNAs (0.5 μl) was transformed into Endura ElectroCompetent Cells (Lucigen, Middleton, WI, USA) according to the manufacturer's protocol, using a Gene Pulser II Electroporation System (BioRad, Hercules, CA). Subsequently, 87 transformations were performed, and the transformants were then plated on LB-agar plates (25 cm × 25 cm) with ampicillin (100 μg/ml). Finally, we obtained 0.8×10^7 colonies from 87 plates, equivalent to 200× coverage for the 39,591 individual sgRNAs. Colonies were collected by scraping the plates, washed with PBS (50 ml), and centrifuged at 4,000 ×g for 10 min at 4 °C to remove the supernatant. The mass of cells per plate was then measured and adjusted to 0.25 g/ml with PBS. Each 80 mg cells per plate were mixed together and resuspended homogeneously. Plasmid DNA from mixed cells were then prepared using the PureYield Plasmid Midiprep System (Promega, Madison, WI, USA), and further purified using a 1% agarose gel to remove contaminating genomic DNA. The purified 50 μl DNA samples (100 μg/ml) were aliquoted and then stored at -80°C for later use. Finally, the sgRNA library targeting 39,591 positions was prepared in the form of a plasmid pool.

Generation of antibiotics treated populations

Purified sgRNA library plasmids (100 ng) were transformed into *E. coli* K-12 MG1655 competent cells containing the pdCas9 plasmid through electroporation. The cells were recovered for 1 h in 2 mLl of SOC media at 37°C and then spread on pre-warmed LB plates

(25 cm × 25 cm) containing chloramphenicol (35 μg/ml) and ampicillin (100 μg/ml) and incubated for 14 h at 30 °C. Finally, we obtained a total of 2.0×10^6 colonies (equivalent to 50× coverage) from 24 plates in the same manner as the above-mentioned sgRNA library preparation. Equal-weight cells per plate were collected together and resuspended homogeneously in 25 ml of PBS. Then, cells were aliquoted into 1 ml and stored at -80 °C with glycerol for later use. For liquid culture, cells were inoculated to OD_{600} 0.05 in LB medium containing chloramphenicol/ ampicillin antibiotics for plasmid maintenance, and pre-cultured up to OD_{600} 1.0. Then, pre-cultured cells were re-inoculated to an OD_{600} 0.05 in 50 ml LB medium or LB media with antibiotics containing a sublethal dose of antibiotics (Table S3), and cultured shaking with 250 rpm at 37°C until the required cell density was achieved.

sgRNA library sequencing

Each sgRNA plasmid was purified from the cell population using the PureYield Plasmid Midiprep System. To construct the sequencing library, plasmids were amplified using TruSeq-based primers containing index and adapter sequences (Table S5). Library amplification was monitored using real-time PCR and SYBR Green, and amplification was terminated at a semi-plateau (typically 18–20 cycles) using an initial 50 ng of plasmid. The amplified library products were separated by agarose gel electrophoresis and purified using a MinElute Gel Extraction Kit (Qiagen, Hilden, Germany). Purified libraries were quantified using a Qubit 2.0 fluorometer (Invitrogen) and sequenced using an Illumina HiSeq 2500 system (Illumina, San Diego, CA, USA). Raw reads were mapped to the *E. coli* MG1655 reference genome (NC_000913.3) using the CLC Genomics Workbench (CLC Bio, Aarhus, Denmark), with a length and similarity fraction of 0.9. The number of reads fall onto each gRNA were counted (Table S1) and ratio of gRNA abundance compared to initial library was calculated. The enrichment ratio (ER) was determined as the median of all gRNA abundance ratios in a gene (Table S2).

Measuring fitness effect of knockout strains

To test fitness effect of genes against antibiotics, knockout strains from the KEIO collection were used. *E. coli* K-12 BW25113, the parental strain for KEIO knockout strains and a close relative of *E. coli* K-12 MG1655, were used as the wild-type control. Growth profiles were monitored using a Synergy H1 microplate reader (Agilent). Fitness effect of each antibiotic was calculated by ratio of area under the growth curve (AUC) under antibiotic stress to AUC without antibiotics.

QUANTIFICATION AND STATISTICAL ANALYSIS

Quantification of gene fitness

The enrichment ratio (ER) of a gene is the median of abundance changes of all sgRNAs targeting that gene. The abundance change of each sgRNA was calculated by dividing its mean abundance (reads per million mapped reads) from two replicate measurements under a given condition by its mean abundance in the initial library. Genes with ER change over 1.5-fold with mean ER (treatment and untreated LB control) larger than 0.25 were regarded as having significant fitness effects against antibiotics. Fitness effects of individual knockout strains under antibiotic stresses were represented by calculating the AUC. Values reported in the figures represent the mean ± SD of three biologically independent experiments.

Statistical analysis

Two-sided Welch's *t*-test (*t*-test with unequal variance) was performed to examine the difference in growth profiles. p-values < 0.05 were considered statistically significant. All statistical analyses were performed using Microsoft Excel. The statistical details of experiments can also be found in figure legends.